BEAM DYNAMICS DESIGN OF J-PARC LINAC HIGH ENERGY SECTION

Masanori Ikegami, Takao Kato, Shuichi Noguchi, KEK, Tsukuba, Ibaraki 305-0801, Japan
Hiroyuki Ao, Tomohiro Ohkawa, Akira Ueno, Kazuo Hasegawa,
Yoshishige Yamazaki, JAERI, Tokai, Ibaraki 319-1195, Japan
Noriyosu Hayashizaki, TIT, Meguro, Tokyo 152-8550, Japan
Valentin V. Paramonov, INR RAS, Moscow 117312, Russia

Abstract

Recently, the beam dynamics design of the high-energy part of J-PARC linac has been revised to reduce construction cost. The modifications are described in this paper together with 3D particle simulations results for the revised design.

INTRODUCTION

ACS (Annular-Coupled Structure linac) is the high-energy part of the J-PARC linac, which accelerates 190-MeV negative hydrogen beams up to 400 MeV [1, 2]. Recently, the beam dynamics design of the ACS part has been improved to reduce construction cost. The beam matching section between preceding SDTL (Separate-type Drift Tube Linac) and ACS is also revised correspondingly. The modifications of the design are described in this paper together with 3D particle simulation results for the revised design.

As presented in the reference [1], we start beam commissioning with lower linac energy of 181 MeV, in which the ACS part is replaced with a beam transport line compatible with swift energy upgrade to 400 MeV. Simulation results for the lower energy operation is also presented.

REVISED ACS

Figure 1 shows the layout of a revised ACS module, which consists of two ACS tanks connected with a bridge coupler, and quadrupole doublets placed at inter-tank spacings. Two neighboring ACS tanks are driven by a 2.5-MW klystron. The inter-tank spacing is $4.5\beta\lambda$ with β and λ being the beam velocity scaled by the speed of light and the RF wave length, respectively.

In the original design [3], ACS part consisted of 46 ACS tanks, and each ACS tank had 15 accelerating cells. The total length including inter-tank spacing was 108.3 m.

In the revised design, the number of ACS tanks is reduced from 46 to 42. To maintain the total energy gain, the number of accelerating cells in an ACS tank is increased from 15 to 17. With this design change, the number of klystrons is reduced by two, curtailing the margin for RF power by around 5 %. The averaged field strength E_0 is reduced from 4.26 MV/m to 4.12 MV/m to keep the increase of RF power load in the sustainable range. The total length of the ACS section is slightly reduced to 107.1 m. Cell geometries of an accelerating cell and a coupling cell are not modified. Bridge couplers are placed below the quadruople doublets in the inter-tank spacing, while we originally plan to place them above the beam line. This layout is selected to enable easy handling of beam instrumentation installed in the inter-tank spacing. Table 1 summarizes the main specifications of the revised ACS.

Table 1: Main specifications of the revised ACS

Input beam energy	190.8 MeV
Output beam energy	400.0 MeV
Operation frequency	972 MHz
Beam particle	Negative hydrogen ion
Peak beam current	50 mA
Beam pulse width	0.5 msec
Repetition	50 Hz (25 Hz initially)
Num. of cells per tank	17
Num. of tanks per module	2
Num. of modules	21
Num. of klystrons	21
Inter-tank spacing	$4.5\beta\lambda$
Bore radius	20 mm
Average accelerating field E_0	4.12 MV/m
Synchronous phase	-30 deg
Max. surface field	0.82 Kilpatrick
Peak RF power	42.5 MW
Peak wall loss	32.0 MW
Peak beam loading	10.5 MW
Total length	107.1 m

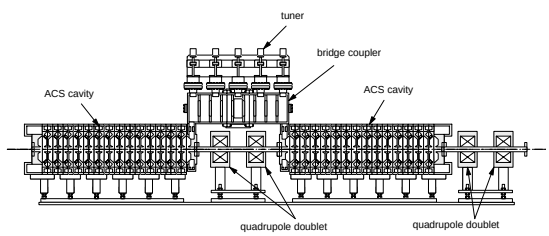

Figure 1: Layout of a revised ACS module. Although the bridge coupler is shown above the beam line in this figure, we plan to place it below.

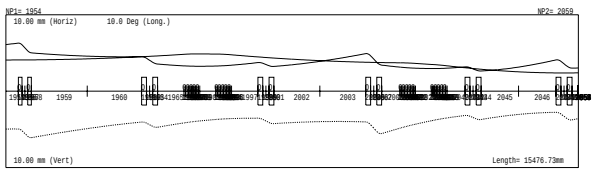

Figure 2: Trace3D output for the revised MEBT2.

Table 2: Normalized rms emittances (400-MeV operation)

	ϵ_x πmm·mrad	ϵ_y πmm·mrad	ϵ_z πMeV·deg
RMS			
RFQ exit	0.205	0.206	0.115
SDTL exit	0.298	0.300	0.149
ACS entrance	0.289	0.288	0.168
ACS exit	0.309	0.312	0.157
RCS injection	0.319	0.294	0.368
99.5 %			
RFQ exit	2.155	2.158	1.556
SDTL exit	4.327	4.558	2.406
ACS entrance	4.407	4.156	2.517
ACS exit	4.827	5.065	2.416
RCS injection	5.173	4.720	5.207

REVISED MEBT2

We have a beam matching section between SDTL and ACS to which we refer as MEBT2 (Medium Energy Beam Transport 2). The main purpose of this beam transport line is to realize smooth matching absorbing the effects of three-fold frequency jump from SDTL (324 MHz) to ACS (972 MHz).

For the longitudinal matching, we have two 972-MHz buncher cavities of ACS-type. A buncher module consists of two 5-cell ACS tanks connected with a short bridge coupler [2, 3, 4]. For the transverse matching, we have six quadrupole doublets. While both SDTL and ACS have doublet-focusing lattices, their period lengths are different. To absorb the difference smoothly, we adopt a "quasi-doublet focusing lattice" for MEBT2, in which the period length is gradually reduced. As the period length in the ACS has been changed from $12\beta\lambda$ to $13\beta\lambda$, the layout (spacing between quadrupole doublets) has been changed accordingly. With this modification, the total length of MEBT2 is reduced from 15.9 m to 15.4 m.

Figure 2 shows a typical beam profile along MEBT2 calculated with Trace3D [5], where middle four quadrupole doublets are mainly used for the transverse matching.

PARTICLE SIMULATION

In this paper, particle simulations are performed with PARMILA [6] from the exit of RFQ to RCS injection. In the simulations, we assume the peak current of 50 mA,

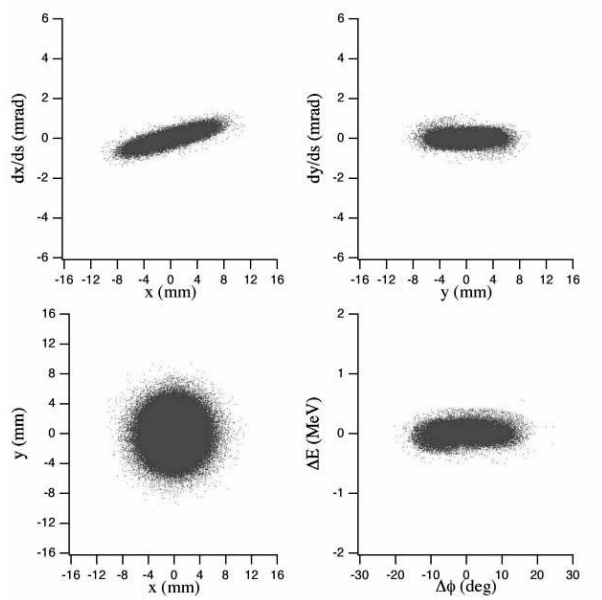

Figure 3: Phase-space distributions at SDTL exit (400-MeV operation).

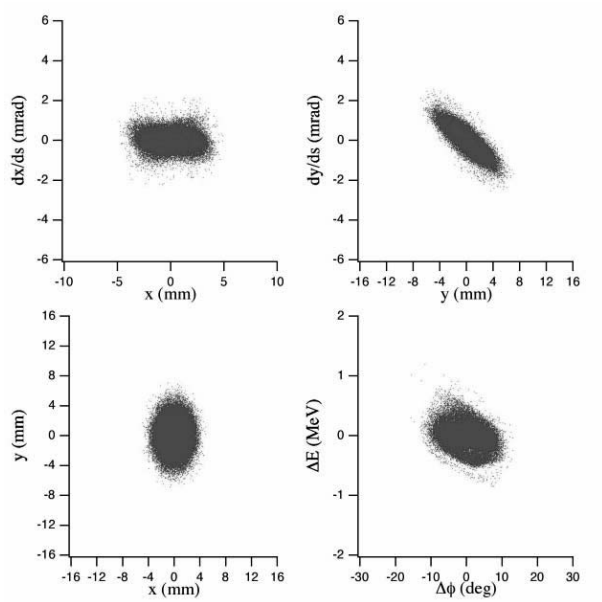

Figure 4: Phase-space distributions at ACS injection (400-MeV operation).

which is the design value for our linac. The initial distribution at the exit of RFQ is obtained with PARMTEQM with the similar procedure described in the reference [7]. The number of simulation particles is 94,720 and the number of meshes is set to 20x20x40. We use the 3D space-charge option. Equipartitioned setting has been assumed for the quadruple magnets in DTL, SDTL, and ACS sections, and no error has been applied.

Table 2 summarizes the evolution of the emittance along the linac, in which phase deviation is measured for 324

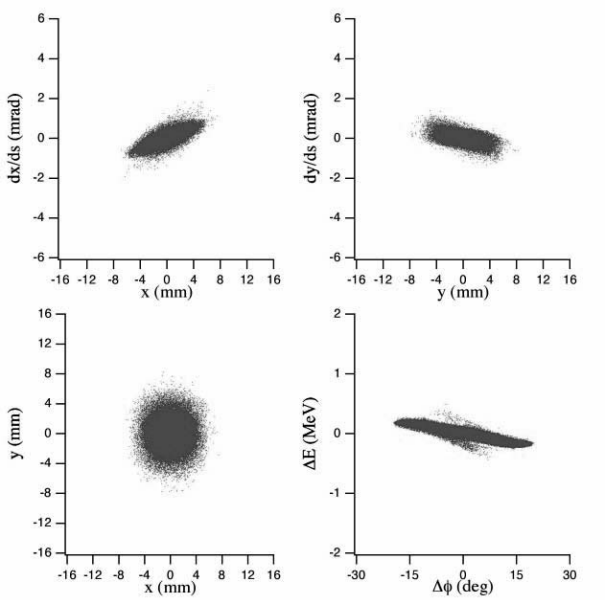

Figure 5: Phase-space distributions at RCS injection (400-MeV operation). The horizontal axis for the right-bottom figure is the phase deviation for 324 MHz.

MHz. As shown in Figs. 3 and 4, slight distortion of the longitudinal distribution occurs in MEBT2. However, the final distribution satisfies the requirement for the momentum spread at RCS injection, ± 0.1 %, as seen in Fig. 5. In the beam transport line from the linac to RCS, the bunch has been rotated in the longitudinal phase-plane to minimize the momentum spread with two 972-MHz debunchers located before and after the 90-degree arc section.

PARTICLE SIMULATION FOR LOWER ENERGY OPERATION

As we start beam commissioning with the beam energy of 181-MeV [1], the lattice design of the high-energy part should be compatible with the lower energy operation. To see its compatibility, PARMILA simulation has also been performed for the 181-MeV operation, where ACS is replaced with a beam transport line. The design consideration of the ACS has been deeply related to the design of the substituting beam transport line, because the capability of swift installation of ACS modules is required to minimize the accompanying beam shut-down period. For the detailed design of the beam transport line, refer to the reference [1].

The simulation conditions are the same with those for 400-MeV operation except that the beam current is assumed to be 30 mA (design value for 181-MeV operation) and the number of particles is slightly increased to 95,322.

Table 3 summarizes the evolution of the emittance along the linac. Figure 6 shows the obtained phase-space distributions at the injection point to RCS. From these results, we have concluded that the revised ACS and MEBT2 satisfy the requirement for the lower energy operation.

Table 3: Normalized emittances (181-MeV operation)

	ϵ_x πmm·mrad	ϵ_y πmm·mrad	ϵ_z πMeV·deg
RMS			
RFQ exit	0.212	0.212	0.0913
SDTL exit	0.262	0.260	0.0958
RCS injection	0.275	0.254	0.262
99.5 %			
RFQ exit	2.075	2.048	1.323
SDTL exit	4.015	3.838	1.370
RCS injection	4.322	3.754	4.078

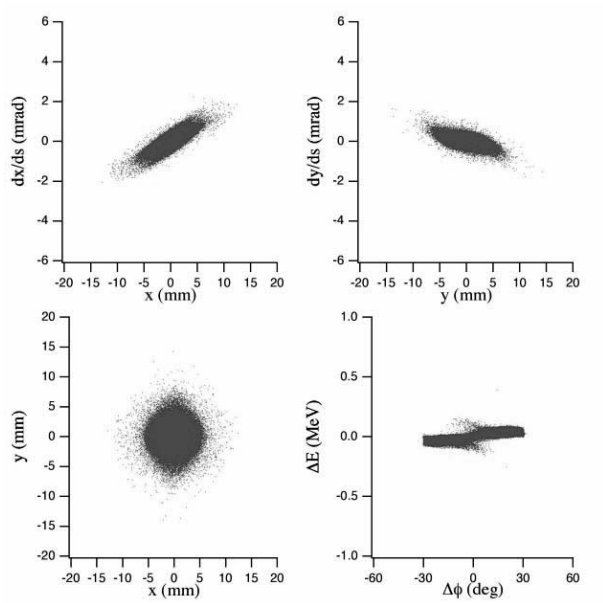

Figure 6: Phase-space distributions at RCS injection (181-MeV operation). The horizontal axis for the right-bottom figure is the phase deviation for 324 MHz.

REFERENCES

[1] Y. Yamazaki, "Status of the J-PARC Linac, Initial Results and Upgrade Plan", in these proceedings.

[2] Y Yamazaki ed., "Accelerator Technical Design Report for J-PARC", KEK Report 2002-13; JAERI-Tech 2003-044.

[3] M. Ikegami et. al., "Beam Dynamics Design of the Annular-Coupled-Structure Lianc and Its Beam Matching Section for the KEK/JAERI Joint Project", in Procs. of LINAC2002, p. 631 (2002).

[4] H. Ao et.al., "Cold-model Tests and Fabrication Status for J-PARC ACS", in these proceedings.

[5] K. R. Crandall, "TRACE: An Interactive Beam Dynamics Code", in AIP Conference Procs. **177**, p. 29 (1988).

[6] H. Takeda, "PARMILA", Los Alamos National Laboratory Report, LA-UR-98-4487 (1998).

[7] Y. Kondo et.al., "Particle Distribution at the Exit of the J-PARC RFQ", in these proceedings.